6th BSME International Conference on Thermal Engineering (ICTE 2014)

Stability of weak confined wake behind a cylinder in fully developed turbulent channel flow

T Vijaya Kumar[a], P.K. Sen[b]*, S.V Veeravalli[b] and Munendra Kumar[a]

[a]**Delhi Technological University, Delhi 110042, India**
[b]**Indian Institute of Technology Delhi, New Delhi -110016, India**

Abstract

The motivation for the study of instability of turbulent wake flow in a confined turbulent channel was multi-fold. First, the instability of confined wake flows has not been studied much. Second, confined wakes are found to retain their mean velocity profile for a considerable downstream distance. Third, wakes have two points of inflection, one each on either side of the centre line. The basic aim of the present study was to investigate the correlation between the turbulence in the wake region and the inflection points in the wake region using stability theory. The wake behind a cylinder of diameter d in a turbulent channel with half width h, is a weak confined wake when $d/h \approx 0.2$. Thus, $d/h = 0.2$ was chosen for the present work. Experimental results are obtained by introducing organized disturbances in the wake and tracking these downstream. Theoretical results were obtained by solving the Orr-Sommerfeld equation by numerical methods.

Keywords: Stability theory; weak wake; inflection point; Karman vortices; turbulence tuner

1. Introduction

The basic task of hydro-dynamic stability theory is to explain all possible phases of transition from the laminar flow regime into the turbulent one in various dynamic systems of fluid mechanics. For near wall turbulence, the process of formation of lift-up and bursting of streaks has qualitative similarity to that of transition in a macroscopic perspective. This, and other examples like free shear flows, lead to interest in study of turbulence by asking the question: Are hydrodynamic instability mechanisms relevant in turbulent flows? In this context researchers have

* Corresponding author. Tel.: +91 9810846032
  E-mail address: pksen@am.iitd.ac.in; pksen45@hotmail.com

explored stability theory for studying some aspects of turbulence. Our present study focuses on a confined weak wake in fully developed turbulent channel flow.

The main difference between wakes and other flows, like wall bounded flows, and other free shear flows, is the presence of the Karman vortex street which persists as the primary feature of disturbance in the flow even in the turbulent regime. Compared with wall bounded flows, free shear flows are highly unstable due to the presence of inflection point in the velocity profile and the associated inviscid instability.

A weak wake is one wherein the minimum velocity is only 10% smaller than the maximum velocity, that is where the maximum defect of the velocity is around 10% of the free stream velocity. Different sizes of cylinders were tried in the turbulent channel and it was found that if the cylinder diameter d is large as compared to the channel width (e.g. $d/h = 0.4$) the Karman vortices help in quickly filling up the wake and even within a downstream distance of $10d$, the wake ceases to exists.

When the cylinder diameter was $d= 8mm$, i.e. 10% of the channel width, a weak wake defined as above was obtained, which persisted for a long distance in the downstream direction. The experimental and the theoretical efforts in the present work was to study the stability of this wake to organised disturbances, and also study its capacity to sustain turbulence. Thus the propagation of organised disturbances along this wake was studied.

Nomenclature

C	Constant	h	Channel half width
Re	Reynolds number	R_{flow}	Flow Reynolds number
U_o	Centreline velocity	U	Instantaneous velocity
$\overline{U}$	Mean velocity	F_{11}	Longitudinal spectrum
F_{1R}	Cross-spectrum	$c=c_r+\iota c_i =\beta/\alpha$	Wave speed, complex
c_r	Wave speed, real	c_g	Group velocity
x	Down stream distance	$x^* = x/\sigma$	Normalised downstream distance
y	Distance across the channel from the wall		
u,v,w	Velocity fluctuations		
$\hat{u}(y)$	Amplitude of fluctuation velocity from Orr-Sommerfeld (OS) solution		
$\tilde{u}$	rms velocity component due to organized disturbance		
U_{rms}	rms velocity of turbulence in the presence of cylinder		
U_{rmso}	rms velocity of turbulence in the absence of cylinder (free stream turbulence)		
$u_r= \sqrt{(U_{rms}^2 - U_{rmso}^2)}$	Excess rms velocity of turbulence in the wake		
σ	Half width of Gaussian distribution , distance from inflection point to centre of channel		
α	Wave number	$\beta = 2\pi f$	Circular frequency
$\beta = \beta_r + \beta_i$	Complex frequency		
μ	Dynamic viscosity	ρ	Density
θ	Phase angle	ψ	Disturbance stream function
ϕ	Amplification function of ψ	rms	Root mean square

2. Relevant Literature

The connection between stability theory and turbulent shear flow was first studied by Landau [1] based on a nonlinear stability model; however this model did not prove to be a suitable model for turbulence. Next, Malkus [2] studied the role of the turbulent mean velocity profile in the Orr-Sommerfeld equation. He proposed that if the mean velocity profile typical of wall-bounded turbulent flows is used in the solution of the classical Orr-Sommerfeld equation, then the profile would prove to be marginally or neutrally stable at the existing Reynolds number. Reynolds & Tiederman [3] proved that the Malkus theory was not valid by performing detailed calculations for a fully developed channel. Later on Reynolds continued work in the area of stability theory applied to fully developed wall turbulence along with Hussain, Hussain & Reynolds [4-5-6]. Initially they started with experiments by introducing controlled, weak, organised disturbances in a fully developed turbulent channel. Reynolds & Hussain [7] also did the theoretical investigations for this problem. Based on their three-way decomposition, they derived the disturbance equation as an extended Orr-Sommerfeld equation. However, neither theoretically nor

experimentally did they find any region of instability.

After Reynolds & Hussain, the problem was untouched for nearly thirty years. Sen & Veeravalli [8-9-10] studied this problem of relevance of hydrodynamic stability theory in understanding wall bounded flows, and they modelled the near wall region with anisotropy, and, theoretically they did observe the existence of Tollimen-Schlichting (TS)-like unstable modes. They found the region of instability to be outside the (stable) region of the theoretical and experimental results studied by Reynolds and Hussain [7], which is possibly why Reynolds and Hussain did not discover the unstable modes. Joshi [11] and Sen, Veeravalli & Joshi [12] compared the theoretical predictions of Sen et al [8-9-10] to their experiments using organised disturbances a fully developed turbulent channel and found that the results matched fairly well.

The works in the area of confined wakes are not many. Shair, Grove, Petersen and Acrivos [13] did experiments to study the effect of confining walls on the stability of a steady wake behind a circular cylinder and found that the stability is greatly enhanced with an increase of *d/h* from 1/20 to 1/5. Barkley [14] carried out a two-dimensional linear instability analysis for the mean flow in the wake of a circular cylinder and found that the eigen frequency of the mean flow tracks the Strouhal number of vortex shedding, almost exactly. The present work goes much beyond these results.

3. Objective and Methodology

The main objective of the present work was to study the evolution of organized disturbances in a weak confined wake both experimentally and numerically, with a view to elucidate the instabilities that arise in such a flow.

As mentioned above, the experiments were conducted in a rig specially designed to yield fully developed turbulent channel flow. Theoretical support for the results was provided by studying the stability of the confined wake profile using the standard Orr-Sommerfeld equation with the appropriate boundary conditions

Table 3.1: Typical flow parameters for the experiments

Centreline velocity	U_o	6.00 *m/s*
Channel half width	h	0.04 *m*
Reynolds Number, $\frac{U_o h}{\nu}$	*Re*	14,200

4. Experimental Setup and Instrumentation

A 2D turbulent channel (wind tunnel) of length 12.2 m and cross section 1.08 m x 0.08 m at the test section was used for the experiment. The walls (vertical) of the tunnel are made of 12 mm thick float glass. A plenum section consisting of several screens, a honeycomb, a 4.8:1 contraction and a small diverging section (to ensure rapid transition from laminar to turbulent flow) is present upstream of the test section. A more detailed description of the channel may be found in Joshi [11]. The organised disturbance is generated by a speaker and introduced into the flow through a slot of 1.5 mm width and 0.1m length, centred in the span-wise direction. The location of the slot was sufficiently downstream of the start of the test section to ensure the existence of fully developed turbulent channel flow. The schematic diagram of the setup and the coordinate system used are shown in figure 4.1. Typical flow parameters for the experiments are listed in Table 3.1.

The arrangement used to perturb the flow with a sinusoidal disturbance, without affecting the mean velocity profile in the wall region, is the same as that used by Joshi [11]. The speaker (ENBEE, 8Ω, 100W) was excited at the desired frequency using a function generator (Aplab, 1Mhz, Model: FG7MD). Velocity measurements were made with a hot-wire probe (Dantec 56C01; 5μm diameter Tungsten wire, approximately 1mm long) connected to an anemometer (TSI IFA 300). The output of the anemometer was suitably amplified and filtered before digitising using an a-to-d card (NI PCI 6143; 16bit) and then stored on a computer for processing. The output of the function generator was also digitised and stored to enable phase-locked averaging of the velocity signal.
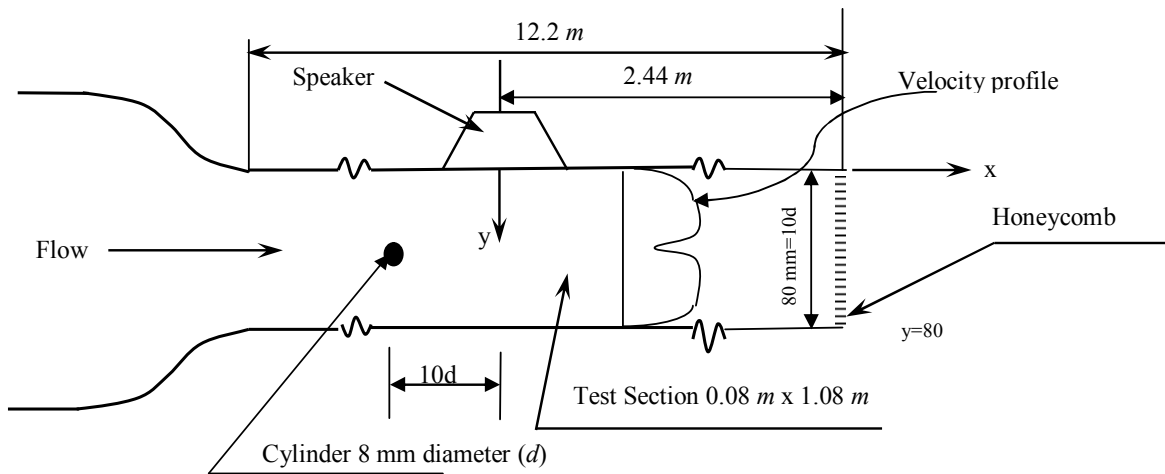
Figure 4.1: Definition sketch for the flow. The typical wake velocity profile and the coordinate system used are also shown.

5. Results and Discussion

5.1 Mean Velocity Profile

Measurements of the turbulent mean velocity profile in the wake region at different downstream distances from the cylinder are shown in Figure 5.1. The channel centerline velocity without the cylinder was approximately 6m/s. To account for minor changes in the ambient temperature and flow conditions, the profiles were scaled to match at one location (y=39mm). It is seen that all the profiles collapse well, indicating that the wake is virtually from $x = d$ to approximately $x = 20d$.
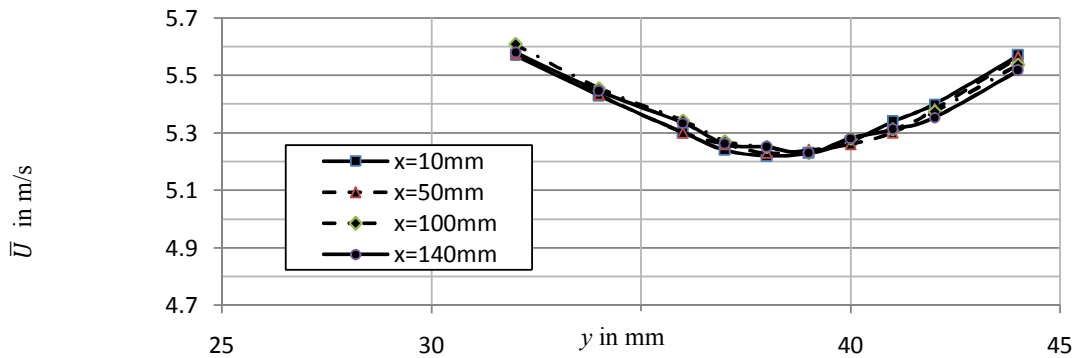
Figure 5.1: Experimental mean velocity profiles for various downstream distances, in the vicinity of the centreline.

The mean velocity profile obtained experimentally was modelled using a combination of parabolic and Gaussian profiles. The location of the inflection point was fixed by suitably selecting the standard deviation σ of the Gaussian distribution as shown in figure 5.2. In the present case σ=0.115, and figure 5.2 shows a perfect match of turbulent mean velocity profile and the synthesized mean velocity profile, in the wake region.

Theoretically, the mean velocity profiles for various downstream distances were obtained by spatial marching of the Navier Stokes equations with the theoretical mean velocity profile of wake. In this analysis the flow was assumed to be laminar. Figure 5.3 shows that the change in profile is insignificant.

The stability study focused on the wake region which is shown in solid line while, the rest is shown with a dotted line, in figure 5.2. For applying the boundary conditions the entire profile from wall to channel centre line is needed. The stability associated with the wake flow is an inviscid instability due to the presence of inflection point in the velocity profile, hence its shape outside central region is not important. Thus for the theoretical studies a combination of the Gaussian profile at the centre and the parabolic (laminar) profile elsewhere, is sufficient.
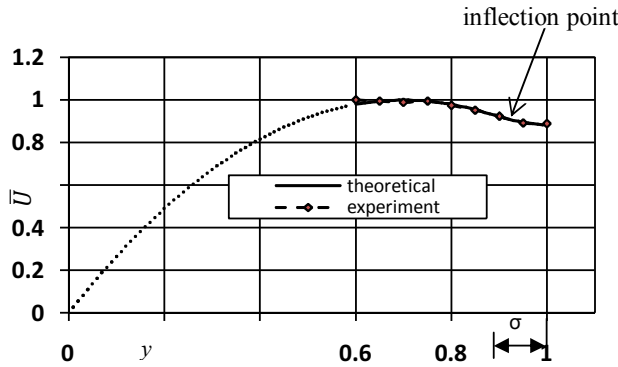
Figure 5.2: Modelling the experimental wake profile using a Gaussian profile (solid line) and a parabola (dotted line).
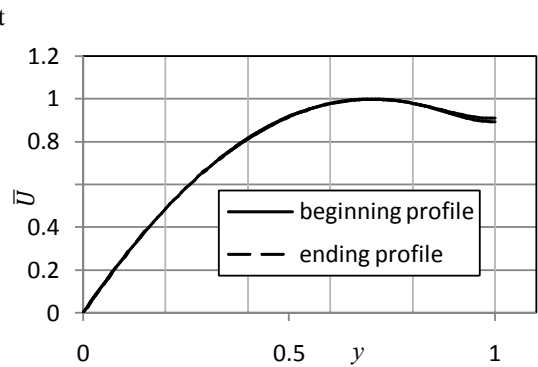
Figure 5.3: Theoretical mean velocity profiles from a calculation spanning the same downstream range as shown in figure 5.1 (i.e. 140mm).

5.2 Theoretical Formulations :-

In linear stability theory, developed by Tollmien and Schlichting, infinitesimal disturbances of a periodic nature are superimposed on the basic laminar flow and their growth rate, which is found to be exponential, is studied. For a primary flow parallel to the x direction, perturbations are assumed to be of the form

$$\psi = \phi(y) \, e^{\, i\alpha(x-ct)}. \tag{5.1}$$

Where $c = \beta/\alpha$, and ψ is the complex disturbance stream function, $\phi(y)$ is the complex amplitude function, α is the spatial wave number, β is the frequency and c is the phase speed.

Inclusion of these perturbations in, and further linearization of the Navier Stokes equations gives the Orr-Sommerfeld equation (5.2) for the complex amplitude function ϕ. Generally, both α and c (or β) would have to be assumed complex implying that an amplitude growing both in space and time is to be considered.

$$i\alpha(\bar{u} - c)(\phi'' - \alpha^2\phi) - i\alpha\bar{u}''\phi - \frac{1}{Re}(\phi''' - 2\alpha^2\phi'' + \alpha^4\phi) = 0 \tag{5.2}$$

The synthesized profile for a weak wake was used in the Orr-Sommerfeld equation and numerically solved for eigenfunctions and eigenvalues to obtain decay/growth rates. The boundary conditions at the wall ($y=0$) are, $\phi = 0$; $\phi' = 0$ and at the channel centre ($y=1$) are: $\phi' = 0$; $\phi''' = 0$, for the symmetric mode and $\phi = 0$; $\phi'' = 0$ for the anti-symmetric mode.

5.3 Turbulence measurements

Next we consider the turbulence levels in the confined wake, in the region where it does not spread. Figure 5.4 shows the turbulence levels (rms value) with and without the cylinder at x =10d. These have been denoted as U_{rms} and U_{rmso} respectively. It is observed from the figure that the turbulence level has gone up more than a factor of four when the cylinder is present. The peak excess turbulence level, u_r, due to the presence of the cylinder may be defined as $\sqrt{(U_{rms}^2 - U_{rmso}^2)}$. Figure 5.5 shows the evolution of u_r with the normalised downstream distance x^* ($x^* = x/\sigma$). It is seen from figure 5.5 that the excess turbulence level decays at an exponential rate.

5.4 Eduction of eigenfunction

2D organised disturbances at various frequencies like 300Hz, 200Hz, 100Hz and 50Hz were used to perturb the flow. The organised disturbance can be extracted from the background turbulence by averaging over a number of cycles at a given phase of the sinusoidal signal obtained from the function generator. While Joshi [11] reports good convergence of phase-locked averages for 10,000 cycles in the wall region, it is seen from Figure 5.6 that for the confined wake, even after 50000 cycles, full convergence has not been achieved. For comparison a pure sine wave is included in this figure.
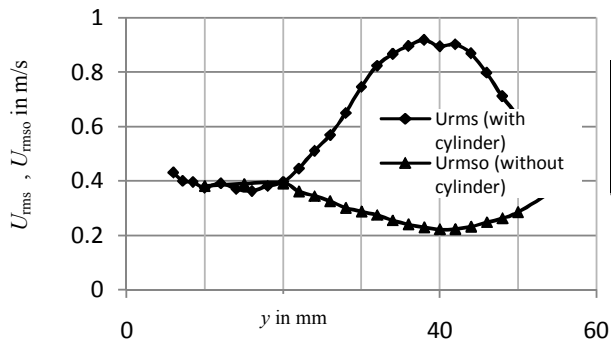
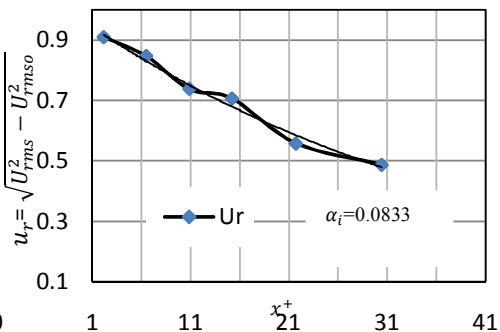Figure 5.4: Comparison of the turbulence levels with and without the cylinder at x/d = 10.

Figure 5.5: Evolution of turbulence excess velocity u_r
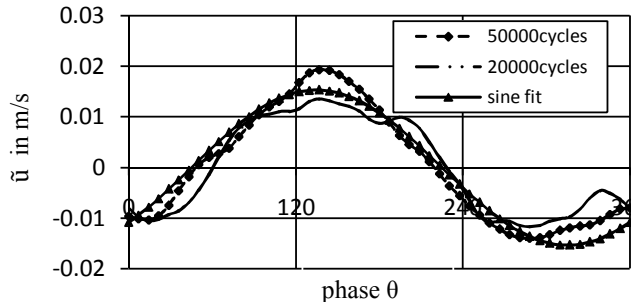

Figure 5.6: Comparison of phase averaging over different numbers of cycles. A pure sine wave is included for comparison.
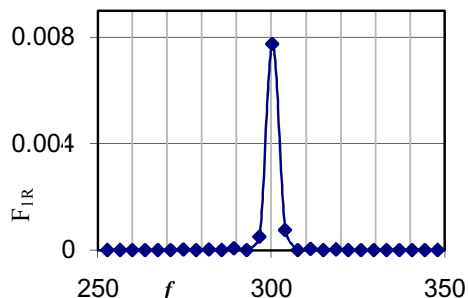
Figure 5.7: Absolute cross spectrum between the turbulence signal and the disturbance signal

One possible reason for this slow convergence is the jittering of mean velocity profile due to the Karman vortices. The presence of two inflection points, one on either side of the centreline also contributes to the problem. Waves originating from either side interfere with each other at a random phase difference and the resulting eigenfunction differs from cycle to cycle. Therefore 5 readings of 50000 cycles at each location were recorded and the average eigenfunction, $\tilde{u}$, was obtained from effectively 250,000 cycles. The average eigenfunction was also obtained from the cross spectrum between the turbulence signal and the disturbance signal. The cross spectrum plot in figure 5.7 shows a spike at the disturbance frequency. The area under the spike gives the magnitude of the eigenfunction, while the phase lag between the output of the function generator and the organised disturbance can be obtained from the imaginary part of the cross spectrum. Figure 5.8 shows a comparison between the eigenfunction obtained from phase locked averaging and the cross spectrum method. As can be seen the match is good.
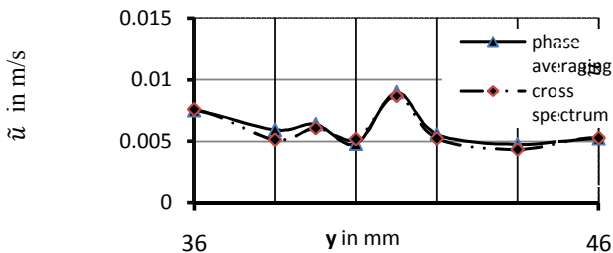

Figure 5.8: The eigenfunction obtained by phase locked averaging and the cross spectrum.
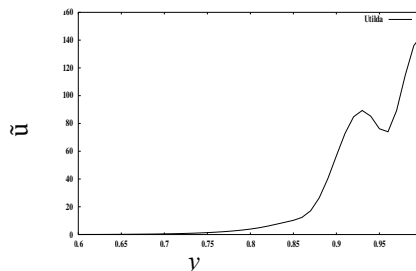
Figure 5.9: $\tilde{u}$ for the anti symmetric ϕ mode

5.5 Theoretical results

Figure 5.9 shows the anti symmetric mode obtained from the solution of the Orr-Sommerfeld equation.. The rms velocity $\tilde{u}_r$ is obtained as $\tilde{u}_r = \sqrt{2\phi\bar{\phi}}$. In figure 5.10 a comparison between the theoretically obtained eigenfunction and its experimental counterpart is shown. The match is good in the central region but the two curves diverge away from the centre. However in the important region (i.e. in the vicinity of the inflection point) the agreement is good.

The computations also indicate that the phase velocity c_r is nearly constant for all values of α, with $c_r \approx \bar{U}_i$ where, $\bar{U}_i$ is the mean velocity at the inflection point. Hence $c_r \approx c_g$ where c_g is group velocity. Hence the growth rate can be estimated as $-\alpha_i = \beta_i/c_r$.
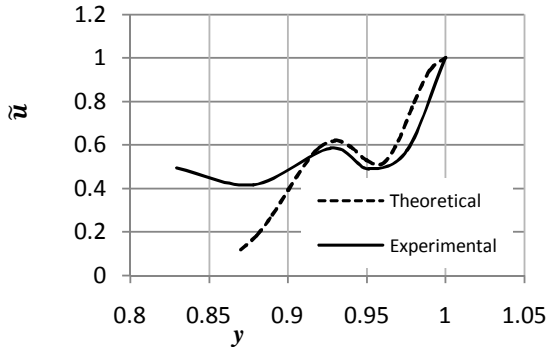

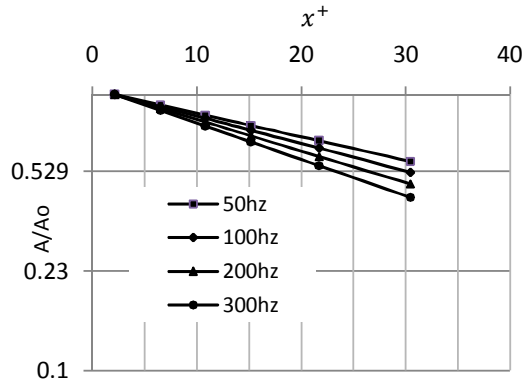Figure 5.10 comparison of experimental and theoretical values of $\tilde{u}$

Figure 5.11: Evolution of the peak value of the eigenfunction . (Theoretical work.)

Figure 5.11 shows the theoretical results for disturbances of various frequencies. The evolution, of the peak amplitude of the eigenfunction, normalised by its initial value at x_o=10 mm (i.e. A/A_o), with the normalised downstream coordinate, x^*, has been shown. Note that $A/A_o = e^{-\alpha_i(x-x_o)}$, hence if the ordinate is shown on a logarithmic scale we expect to see straight lines at each frequency. This is what is observed, further the decay rate is higher at higher frequencies. All the modes obtained from the theoretical calculations were weakly damped at best.

5.6 Experimental Results

As mentioned earlier convergence in the experiments is very slow and hence our estimates of the eigenfunction is likely to possess large scatter. Figure 5.12 (a) shows a typical set of data points obtained for the experimental evolution of the peak ratio, $\tilde{u}/\tilde{u}_o$, along with their error bars. What is shown is the mean value bracketed by twice the standard error estimated. To within experimental error then the data support exponential decay. The data for disturbances at other frequencies shows similar scatter.

Figure 5.12 (b) shows the evolution of $\tilde{u}/\tilde{u}_o$ for several different excitation frequencies. In this figure only the exponential fits are shown. The observation made in the discussion above, with the theoretical results, that the decay at higher frequencies is higher is verified by the experimental data, however, the corresponding decay rates are somewhat higher in the experiments. In Figure 5.12(b) the evolution of the excess turbulence and peak of the eigenfunction obtained without any external excitation, are also shown. The latter labelled 'Karman vortices' has been obtained by disconnecting the speaker but still using a sinusoidal signal of 165Hz (corresponding to the Strouhal frequency) to obtain phase locked averages. Both these data sets also support exponential decay, with the 'Karman vortices' set showing the highest decay rate. This is possibly due to the fact that no excitation was used and therefore in addition to a reduction in the strength of the disturbance there was a loss of coherence with the sinusoidal signal used for phase averaging also.
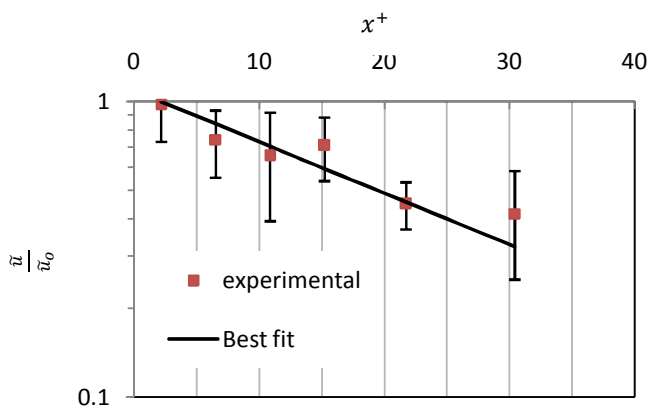

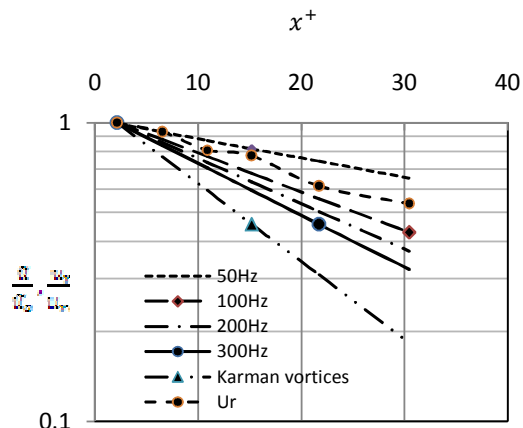*Figure 5.12(a): Variations of $\tilde{u}$ in downstream direction for 300Hz.*

Figure 5.12(b): Variations of $\tilde{u}$ in downstream direction..

5.7 Spectral Analysis

Figure 5.13 shows power spectra of the longitudinal velocity (F_{11}) at centre of the channel for different downstream distances, without the sinusoidal perturbation. There is a spike seen at the Strouhal frequency (165 Hz) when the cylinder is present. The power spectrum plots also show that there is a decay of amplitude in the downstream direction.

From the power spectrum, for frequencies f= 50Hz, 100Hz, 200Hz and 300Hz, (corresponding to the different excitation frequencies) the corresponding densities were picked up and a best fit plot (similar to that of the eigenfunction peak) of the normalised excess spectral density $\frac{A-A_1}{A_o-A_1}$ versus x^+, (where A_o is the spectral density at the first location, x=10mm and A_1 is the value at x=10 mm when the cylinder is not placed) is shown in figure 5.14. These plots too are consistent with the earlier mentioned behaviour that higher frequencies decay faster.
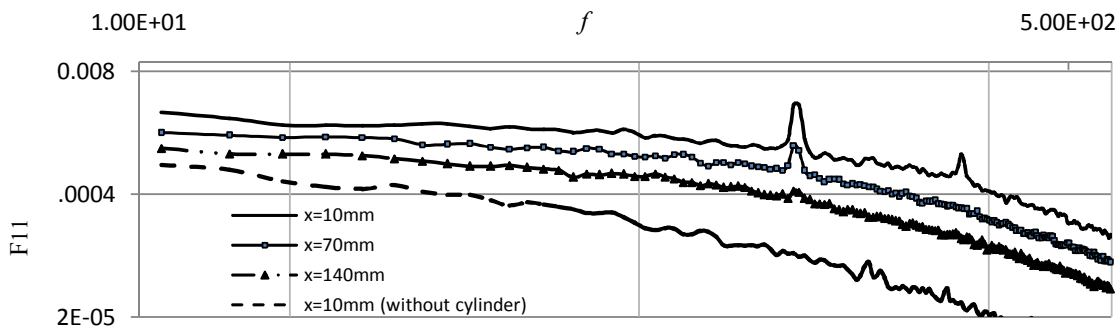

Figure 5.13: Power spectra with and without cylinder at different downstream distances, at y=40mm.
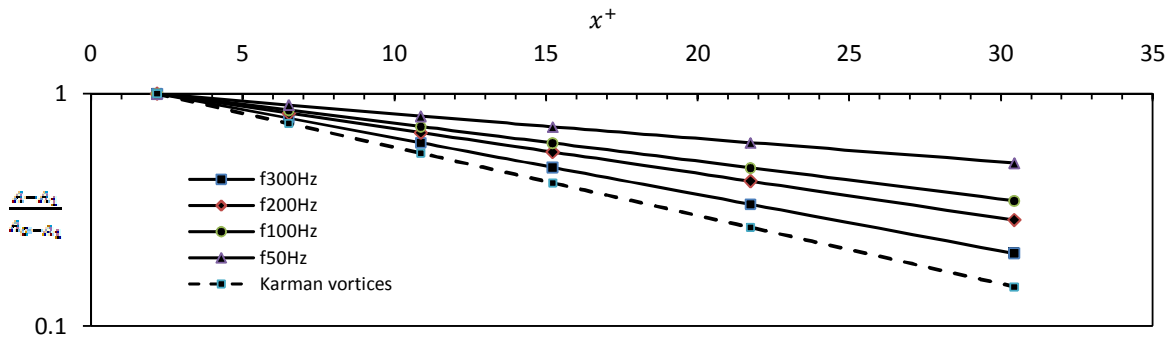
Figure 5.14: Evolution of the normalised excess spectral density in the downstream direction.

6. Conclusions

The mean velocity profile of the weak confined wake is virtually unchanged over a fairly large downstream distance ($x \approx d$ to $x \approx 20d$). Intriguingly this matches well with the theoretical evolution (laminar) wherein the background turbulence is ignored. Thus the confinement of the weak wake appears to exactly counter the spreading expected in the presence of the background turbulence.

The theoretical results indicate that although no unstable modes exist, weakly damped modes are present for a wide range of excitation frequencies. Moreover, the decay rate (exponential) increases with frequency. The theoretically obtained values of c_r are more or less constant and approximately equal to the mean velocity at the point of inflection. Hence, $c_g \approx c_r$, and the spatial growth rate may be obtained as $-\alpha_i = \beta_i/c_r$.

The experimentally determined eigenfunction matches the one obtained theoretically, quite well. Further, both the peak of the eigenfunction and the power spectral density excess exhibit exponential decay and show faster decay for higher frequencies. We note however, that the convergence of the experimental eigenfunction by phase averaging is extremely slow, possibly due to the interference of modes originating from the two inflection points.

7. References

[1]   Landau L .D (1944) On the problem of Turbulence . C.R. Acad. Sci. U.R.S.S 44, 311-314.
[2]   Malkus W. V. R., 1956, Outline of a theory of turbulent shear flow, *J. Fluid Mech.*, 1,521- 539.
[3]   Reynolds W. C., and Tiderman W. G., 1967, Stability of turbulent channel flow, with application to Malkus's theory, *J. Fluid Mech.*, 27, 2, 253-272.
[4]   Hussain A.K.M.F. and Reynolds W.C., 1970, The mechanics of an organized wave in turbulent shear flow, *J. Fluid Mech.,* 41, 2, 241-258.
[5]   Hussain A.K.M.F. and Reynolds W.C., 1972, The mechanics of an organized wave in turbulent shear flow Part 2. Experimental results, *J. Fluid Mech.,* 54, 2, 241-261.
[6]   Hussain A.K.M.F. and Reynolds W.C., 1975, Measurements in fully developed turbulent channel flow, *J. Fluids Eng.*, 97, 568-578.
[7]   Reynolds W.C. and Hussain A.K.M.F., 1972, The mechanics of an organized wave in turbulent shear flow Part 3. Theoretical models and comparison with experiments, *J. Fluid Mech.*, 54, 2, 263-288.
[8]   Sen P.K. and Veeravalli S.V., 1998, On the behaviour of organized disturbances in a turbulent boundary layer, *Sadhana*, 23, 167-193.
[9]   Sen P.K. and Veeravalli S.V., 2000, Behaviour of organized disturbances in fully developed turbulent channel flow, *Sadhana*, 25, 423-437.
[10]   Sen P.K., Veeravalli S. V., Carpenter P. W., Joshi G. and Josan P. S., 2007, Organised structures in wall turbulence as deduced from stability theory-based method, *Sadhana*, Vol. 32, Part 1 & 2, 51-64.
[11]   Ganpati Narasimha Joshi., 2012, Experimental Investigation on the relevance of Hydrodynamic stability theory to wall-turbulence, Ph.D thesis, IIT, Delhi.
[12]   Sen P.K., Veeravalli S. V., Joshi G.,2013, Stability theory and experiments in wall-turbulence, Procedia Engineering 56 (2013), pp. 29-38.
[13]   Shair F. H., Grove A. S., Petersen E.E. and Acrivos A (1963) The effect of confining walls on the stability of the steady wake behind a circular cylinder, *J. Fluid Mech.*, 17, 4, 546-550.
[14]   Barkley D (2006) Linear analysis of the cylinder wake mean flow .Euro physics letters 75(5) 750-756.